Demonstration of Atmospheric-Pressure Radiometer with Nanocardboard Vanes

Mohsen Azadi, Zhipeng Lu, George A. Popov, Christopher H. Stanczak, Andy G. Eskenazi, Pratik Ponnarassery, John Cortes, Matthew F. Campbell, and Igor Bargatin

Abstract-Crookes radiometers have been the subject of numerous theoretical, numerical, and experimental studies because of the complicated forces they exhibit as well as their potential applications to light sensing and actuation. The majority of these studies have focused on classical radiometers, which function under low vacuum pressures. In contrast, here we report a radiometer with microengineered vanes that rotates at atmospheric pressure. Its functionality at pressures thousands of times higher than previous light mills is due to unique attributes of the nanocardboard that forms its vanes: 1) the extremely low areal density (0.1 mg/cm²) of nanocardboard reduces the vane masses by two orders of magnitude; 2) its lower thermal conductivity allows a greater cross-vane temperature difference; and 3) its microchannels dramatically increase the thermal transpiration flow that drives the rotation. Intriguingly, the experimentally observed rotation speeds are substantially higher than those theoretically expected. Our device demonstrates new possibilities for micromanipulation, propulsion of aerial vehicles, and light-powered generators.

Index Terms-Photophoresis, Mechanical Metamaterials, Microfabrication, Radiometer

I. INTRODUCTION

RADITIONAL Crookes radiometers, shown in Fig. 1, are well-known examples of opto-thermo-mechanical coupling [1]. They usually consist of a low-friction hub and four lightweight paper vanes that are colored black and white on opposing faces and are placed inside a glass chamber under low

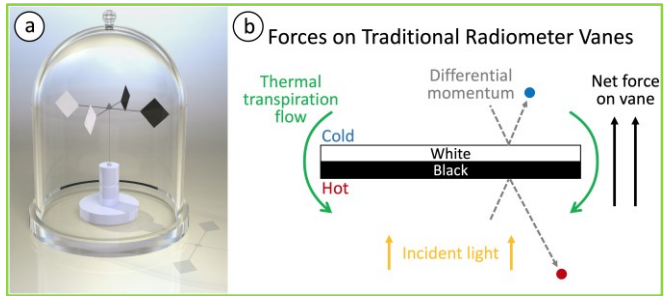


Fig. 1. (a) Photorealistic rendering of a traditional radiometer in a vacuum jar. Light heats the dark sides of the vanes, inducing a photophoretic force that causes the vanes to rotate. (b) Schematic diagram showing forces on traditional radiometer vanes. The differential momentum force arises from molecules departing the light and dark-colored faces with different velocities, whereas the thermal transpiration force arises from gas molecules slipping around the edges of the vanes.

This work was funded in part by a NSF CAREER award under grant CBET-1845933. Also, this work was carried out in part at the Singh Center for Nanotechnology, which is supported by the NSF National Nanotechnology Coordinated Infrastructure Program under grant NNCI-1542153.

M. Azadi, G. A. Popov, C. H. Stanczak, P. Ponnarassery, A. G. Eskenazi, M. F. Campbell, and I. Bargatin are affiliated with the Department of

vacuum (~1 Pa). When exposed to sunlight, the black sides of the vanes are radiatively heated to a higher temperature than the white sides. Two forces arise as a result. First, molecules

impacting the hotter black sides on average depart with higher velocities than those contacting the white sides; this results in a small differential recoil force. Second, as a result of the temperature gradient, gas molecules tend to creep around the edges of the vanes from the white sides to the black sides. This motion, called thermal transpiration, also causes the vanes to move in a direction toward the white sides. However, as the pressure rises above ~10 Pa, both the differential recoil and thermal transpiration forces decrease and eventually become smaller than the static friction and aerodynamic drag forces,

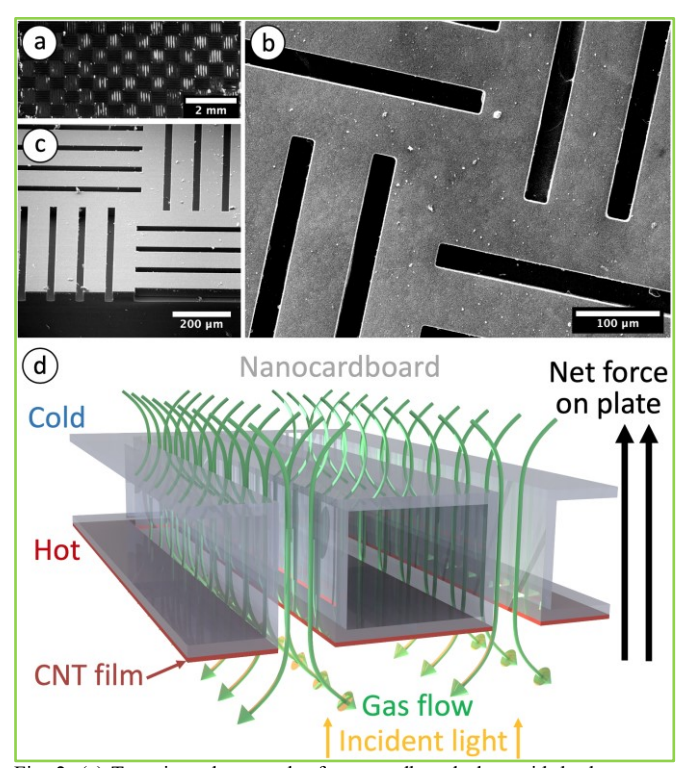


Fig. 2: (a) Top-view photograph of nanocardboard plate with basketweave-style 5-channel unit cell design. (b) Top-view SEM image of nanocardboard channels. (c) SEM perspective-angle image showing height of channels. (d) Schematic diagram showing thermal creep-induced gas flow through nanocardboard channels. Incident light heats the CNT-coated bottom plate, whereas the top plate remains relatively cool.

Mechanical Engineering and Applied Mechanics, University of Pennsylvania, Philadelphia, PA 19104 USA. Z. Lu is affiliated with the Department of Chemistry at the same university, and J. Cortes is affiliated with Lawrence Livermore National Laboratory, Livermore, CA, 94550 USA.

Please direct correspondence to I. Bargatin (tel: +1-215-746-4887; email: bargatin@seas.upenn.edu).

preventing the hub from turning.

Though a wide variety of radiometer geometries have been created, virtually all have been limited to low-pressure operation. For example, Han *et al.* recently constructed a radiometer with curved vanes in order to promote asymmetric heating and operated it at pressures below 13 Pa [2]. Also, Wolfe *et al.* developed a radiometer with horizontal (rather than vertical) vanes in order to explore the relative influence of the differential momentum and thermal transpiration forces that operated at pressures of less than 35 Pa [3]. However, operation at atmospheric pressure would be both interesting from a fundamental point of view and more useful in educational demonstrations. Additionally, photophoretic propulsion may be useful as an alternative locomotion strategy for miniature aircraft, requiring this mechanism to operate in a wider range of pressures [4,5].

For these reasons, we have developed a Crookes radiometer that is capable of rotating at atmospheric pressure because it has vanes composed of a unique material called nanocardboard (Fig. 2) [6]. Nanocardboard is a metamaterial composed of two alumina face sheets of nanometer-scale thickness connected by thin hollow channels. This architecture results in an areal density that is two orders of magnitude lower than traditional paper radiometer vanes, and also provides very high thermal resistance between the face sheets. By applying a thin coating of light-absorbing carbon nanotubes to one of these face sheets and exposing the vanes to light, we can induce a temperature differential of a few kelvins between the face sheets, sufficient to drive a strong thermal transpiration flow through the densely arrayed channels of nanocardboard. These factors work together to amplify the thermal transpiration force on the vanes, allowing the radiometer to function at atmospheric pressure. The following sections explain our methods for fabricating the nanocardboard vanes and the radiometer, present a theory for its operation, show our testing procedure and apparatus, and finally present experimental results.

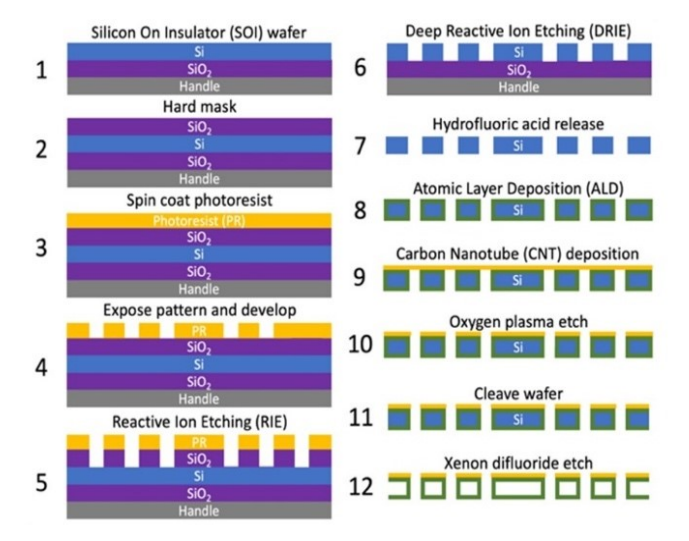


Fig. 3: Vane fabrication process. We create a silicon mold with channels using a combination of RIE and DRIE, release the mold using HF, perform ALD of alumina, deposit CNTs, clean the channels using oxygen plasma etching, and finally release the alumina using XeF_2 isotropic etching.

II. FABRICATION

A. Vanes

We manufactured our radiometer vanes using a sacrificial mold according to conventional microfabrication techniques (Fig. 3) in four phases: 1) mold creation, 2) mold conformal coating, 3) carbon nanotube (CNT) deposition and cleaning, and 4) mold etching.

(1) To fabricate the mold, we began by coating a 10-cm Silicon-On-Insulator (SOI) wafer that had a 60-µm device layer (Ultrasil LLC) with a 2-µm SiO₂ hard mask using plasmaenhanced chemical vapor deposition (Oxford Instruments). We then spin-coated and baked Shipley Microposit S1818 photoresist onto the wafer (1800 RPM for 60 s and 115 °C for 60 s), exposed a pattern to define the vertical nanocardboard channels using a SUSS MicroTec MA6 Gen 3 mask aligner (350 mJ/cm² dose), developed the polymer using MF319 developer (70 s at 20 °C), and baked the result (115 °C for 5 min). Next, we transferred the pattern in the photoresist to the hard mask using CHF₃/O₂ reactive ion etching (Oxford 80 Plus) and subsequently transferred the pattern from the hard mask to the device layer using deep reactive ion etching with SF₆ and C₄F₈ (SPTS Si DRIE). Lastly, to release the molds (16 per wafer), we immersed the wafer in a 49% HF bath for 60 min and removed each using a blade.

(2) To conformally-coat all sides of the molds, we fixed

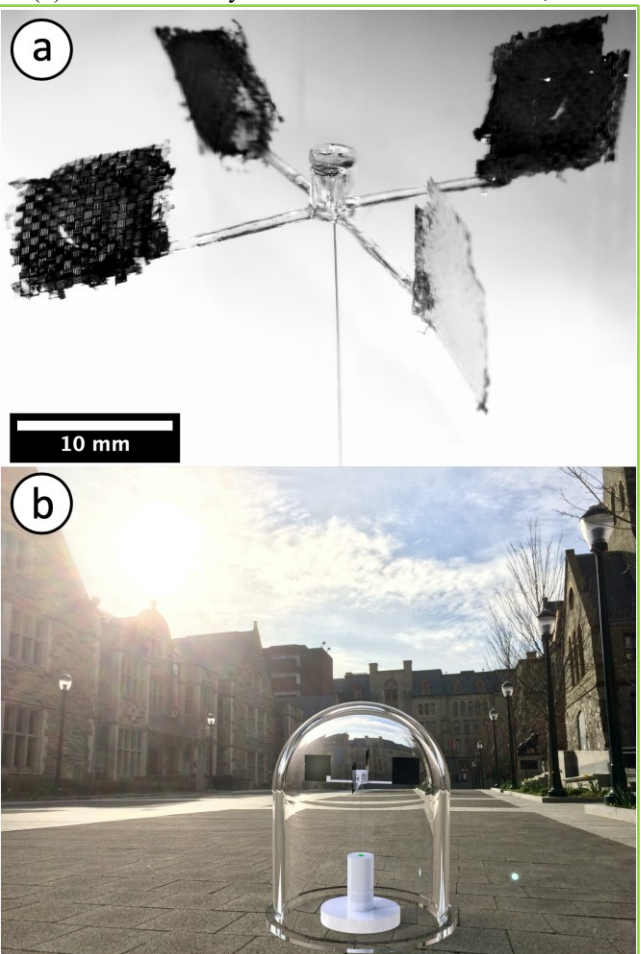


Fig. 4: (a) Photograph of vanes glued the hub, which is balanced on the spindle. The vanes are shown prior to the XeF₂ etch process. (b) Photorealistic rendering of the radiometer under sunlight on the University of Pennsylvania campus. The bell jar prevents wind from moving the vanes.

each to a glass holder using Kapton tape and deposited 100 nm of alumina (Al₂O₃) at 250 °C using atomic layer deposition (Cambridge NanoTech S200). For this process, we used precursors H₂O and Al₂(CH₃)₆ with a 15 ms pulse and 5 s delay for both.

- (3) To deposit the absorptive CNT layer, we dropcasted a solution of single-wall CNTs (0.2% w.t. water, further diluted with water by a 3:1 volumetric ratio) on one side of the aluminacoated molds and placed them on a hot plate at 50 °C to evaporate the water. We repeated this deposition a second time, at which point the absorptivity was approximately 90% [4]. This dropcasting method clogs the nanocardboard channels; to reopen them, we conducted reactive ion etching with O_2 plasma for 2 min on the opposing (non-coated) face of the molds (Oxford 80 Plus).
- (4) The final step in the vane manufacturing process was to etch the silicon mold away from within the conformal alumina coating, leaving only the lightweight, hollow rigid shell. To accomplish this, we used a blade to cut openings in two opposing edges of the molds and conducted 600 cycles of XeF₂ vapor etching (70 s each at 2.5 Torr pressure with a 3 s delay; Xactix SPTS E1). The final mass of each 1.5-cm-square vane was approximately 0.1 mg.

B. Quad-arm hub

We used a ProJet 6000 SLA 3D stereolithography printer to fabricate a 26-mm-diameter quad-arm hub using Accura ClearVue resin. The printing technique allowed us to achieve good rigidity with low mass by constructing the mount as one entity rather creating it by joining several separate pieces, and furthermore ensured that the hub's center of mass was precisely positioned upon its axis of symmetry. The overall size and geometry were chosen to match those of traditional vacuum radiometers.

C. Assembly

We used a minimal amount of superglue (Loctite) to mount the microfabricated vanes onto the hub's arms, and subsequently press-fit a V-shaped sapphire bearing (Swiss Jewel V3.18) into a pocket in the center of the hub. The weight of the hub-and-bearing assembly, measured using a precision scale (Perkin-Elmer AD4), was 56 mg. We placed the hub upon a 120-µm diameter SEIRIN J-Type acupuncture needle that was held vertically and served as the spindle. Our choices of the bearing and the needle were coordinated to reduce the surface area overlap and resulting friction force. Figure 4 shows a photorealistic rendering of the radiometer in a courtyard on the University of Pennsylvania campus, as well as a photograph of the as-fabricated hub and spindle assembly.

D. Chamber

We assembled a light chamber in order to perform repeatable tests of the radiometer's performance (Fig. 5). This rig consisted of an octagon-shaped open-top compartment (47-mm internal side length) with eight LED arrays (LOHAS LH-XP-100W-6000k) mounted to its interior walls and eight thermoelectric coolers (GeeBat TEC1-12706 with Acrylic Silver 5 AS5-3.5G thermal paste) on its exterior. The LED

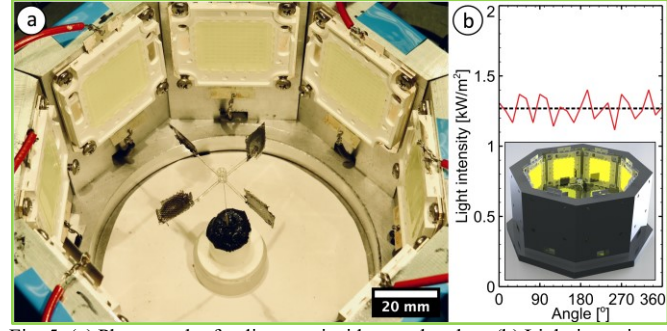


Fig. 5: (a) Photograph of radiometer inside test chamber. (b) Light intensity as a function of angular position within the chamber at a radius of 13 mm. Eight peaks, corresponding to the eight LEDs, can be distinguished. Inset: Computer rendering of chamber showing LED illumination.

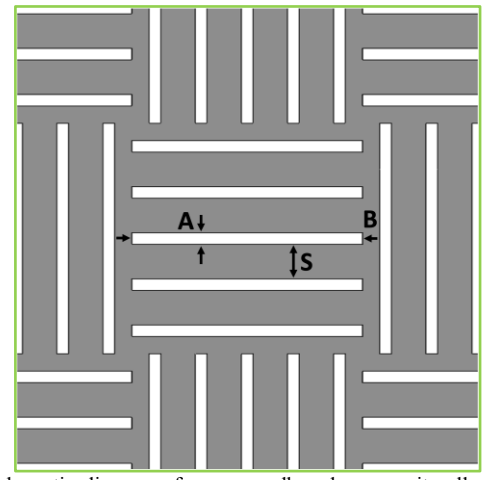


Fig. 6: Schematic diagram of a nanocardboard vane unit cell with X = 5 channels per cell, channel width A, channel length B, and channel spacing S (the channel height L is not shown). See also dimensions in Table I.

arrays, whose brightness we controlled using a current source, provided uniform light intensity in a 26-mm diameter circle within the chamber (~6.5% variation, as measured using a Thorlabs S305C sensor; see Fig. 5), while the thermoelectric coolers mitigated convection flows inside the light chamber. We placed the radiometer inside the chamber along its axis of symmetry. During the experiments, we used a Testo 875i thermal camera to monitor the temperature of the chamber walls, which reached 40-50 °C in the steady state. We placed a 9-cm-diameter cylindrical open-ended polycarbonate tube (McMaster-Carr, Inc. #8585K47) over the assembly within the chamber to provide a quiescent environment free of room air currents, convection from the warm chamber walls, and other disturbances. The open end of this tube allowed us to make undistorted thermal temperature measurements from above. Finally, we used a camera mounted above the chamber to film the rotation of the vanes and used video analysis software to obtain the rotation speed of the hub in each experiment.

III. THEORETICAL MODELING

To understand the air motion near and through the vanes, we employed a fluid mechanical model based on ref. [4]. For brevity, we will present only the most relevant equations here. For a nanocardboard plate that is fully submerged in air and can move freely, the mean gas flow-through velocity in the nanocardboard channels u_{ft} is given by (1),

$$u_{ft} = \frac{\varphi\left(\gamma(T_b - T_f)\right)}{\rho AB} \tag{1}$$

in which T_f and T_h , are the temperature on the front (no CNTs) and back (with CNTs) of the vane (respectively), ρ is the density of the flowing air, A and B are the width and length of the channels, respectively (see Fig. 6 and Table 1), the channel fill factor is

$$\varphi = \frac{4 X A B}{A_{total}} \tag{2}$$

The thermal creep coefficient is given by

$$\gamma = \left(\frac{1.1}{1.5 + \delta}\right) \frac{A^2 B P \beta_*}{2(T_f + T_b)L} \tag{3}$$

In (2), X = 5 is the number of channels in a parallel pattern of the nanocardboard plate and the total unit-cell area

$$A_{total} = (AX + B + S(X+1))^{2}$$
 (4)

depends on the distance S between channels. Equation (3) also uses the total height of the channels L (i.e., the height of the nanocardboard plate), the rarefication factor

TABLE I GEOMETRIC PARAMETERS OF THE UNIT CELL USED FOR VANES DESIGNED IN THE EXPERIMENTS AND NUMERICAL MODELING

Parameters	Value
A	25 μm
B	25 μm 500 μm 75 μm 60 μm
S	75 μm
L	60 μm
X	5

$$\delta = \frac{\sqrt{\pi}}{2} \frac{A}{\lambda},\tag{5}$$

and the inverse of the characteristic gas velocity
$$\beta_* = \sqrt{\frac{m}{k_B(T_f + T_b)}}$$
(6)

where λ is the average mean free path of air molecules, m is the average molecular weight of air, and k_B is the Boltzmann constant. Inserting (2)-(6) into (1), we find that the flowthrough velocity increases with the temperature gradient along the channel walls, which in turn is proportional to the incident optical power $\frac{(T_b - T_f)}{L} \approx \frac{I_{incident}}{2 k_{air}}$, where we use the conductivity of air to approximate the conductivity of hollow nanocardboard. For an incident intensity of 1000 W/m² (= 1 Sun, i.e., the solar intensity on Earth's surface), the flowthrough velocity is on the order of 1 mm/s. This theory and the flow-through velocity values successfully predicted the hovering heights of nanocardboard in our previous experiments at the atmospheric pressure [4]. However, as detailed below, the hub radial velocity values we measured experimentally are about an order of magnitude larger, indicating a possible large

IV. SIMULATIONS

role of fluid-dynamic interactions between the vanes.

In order to understand the fluid dynamics governing the entire radiometer, we conducted numerical simulations using OpenFOAM computational fluid dynamics software. Briefly, we created a three-dimensional model of the radiometer using

solid square planes as vanes and the 3D-printed hub part. Importantly, we filleted the edges of the hub to prevent computational errors and/or discontinuities at its sharp edges and corners. Moreover, we used a control volume to match the dimensions of the polycarbonate tube placed within the chamber. This resulting mesh had approximately 2,000,000 mesh elements. Using this model, we employed the solver SRFSimpleFOAM to solve the complete Navier-Stokes equation for a single rotating reference frame with constant rotation speed, via the SIMPLE algorithm. In these simulations, we specified the relative velocity of the vanes to be normal to the surface and equal to the flow-through velocity and applied a no-slip condition on all the walls and elsewhere. We also set a zero-gradient pressure on all the solid surfaces, except the vanes.

To determine the hub rotation speeds using OpenFOAM, we conducted successive simulations while modifying the flowthrough velocity through parameter sweep, and found the crossover point where the calculated torque on the vanes and hub vanished. Our simulation results indicate that, at low rotation speeds of about 2 revolutions per minute (RPM), the flow fields associated with each vane are essentially orthogonal and do not interfere with one another. However, at higher speeds such as 5 RPM and above, the simulations revealed more complex interactions between the four vanes' velocity fields, as shown in Fig. 7. For rotational speeds that resulted in the interaction of the vanes, the simulations predict bulk movement of the air inside the chamber. To find the simulated flowthrough velocity of individual vanes, we found the average speed of the air for a ring that the vanes sweep when they rotate and then subtracted this speed from the linear velocity of the vanes.

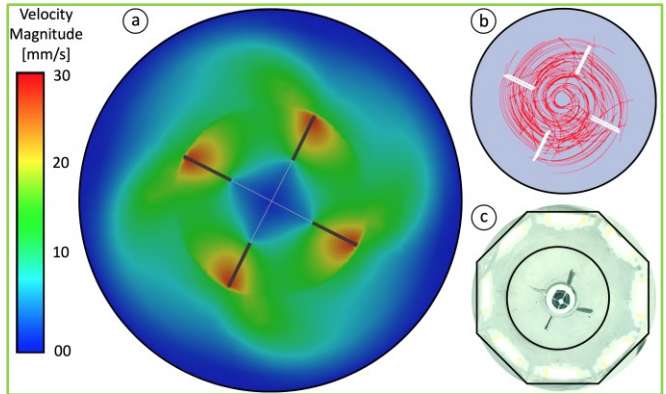


Fig. 7: Top view of the (a) flow field and (b) streamlines in an atmosphericpressure numerical simulation in which the vanes (1.5-cm square in this simulation) rotated at 10 RPM. Notice that the peak velocity values occur near front and back surfaces of the vanes, indicating flow is occurring through the channels. (c) Top-view photograph of the experimental setup, showing the LED illumination. The black circle corresponds to the open-ended polycarbonate tube placed around the radiometer to block room air currents.

V. EXPERIMENTAL RESULTS AND DISCUSSION

We measured the rotation speed of the hub as a function of the light intensity within the chamber, as shown in Fig. 8. As expected, the net forces pushed on the black CNT-coated side of the vanes, and the rotation speed increased with increasing

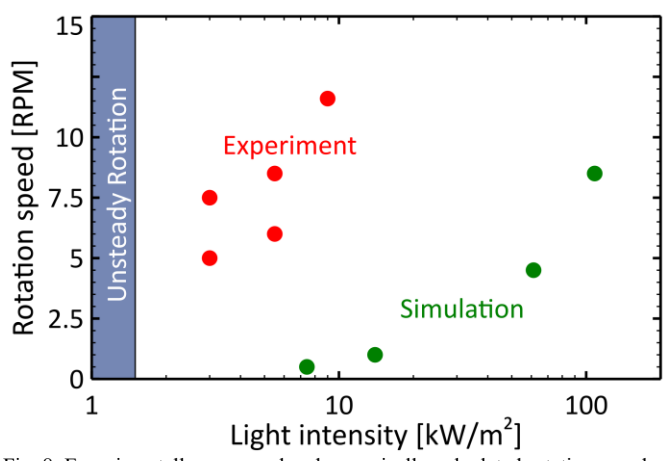


Fig. 8: Experimentally-measured and numerically-calculated rotation speeds as a function of light intensity incident on the vanes. The rate increases with increasing light intensity, indicating a stronger temperature gradient and a higher channel flow velocity within the nanocardboard. The light intensity values at which we observed unsteady rotation was are shaded.

light intensity because of the increasing flow-through velocity, according to (1). We note that the continuous smooth rotation started only at intensities above $\sim 1.5 \, kW/m^2$ and there was no movement below $0.5 \, kW/m^2$. Between these two values, we observed irregular stop-go movements which could be caused by the varying intensity as a function of the angle (see fig. 5), uneven static friction between the spindle and the bearing, and asymmetric distribution of mass (glue, hub, etc).

The maximum rotation speed of 11.6 RPM corresponds to an angular velocity of ~ 1.2 rad/s and linear velocity of the vanes of ~2.5 cm/s, which is about 5-10 times higher than the theoretically expected flow-through velocity in the channels. Using (1), we estimate that the 2.5-cm/s flow-through velocity corresponds to a local temperature gradient of 25 °C between the nanocardboard faces, which is unrealistically high. For a given light intensity, the rotation speeds predicted by the simulations are approximately an order-of-magnitude smaller than those measured in the experiments (Fig. 8). This discrepancy is likely due to an underestimation of the photophoretic forces and flow-through velocity by our theory for vanes that are in mid-air at atmospheric pressure. Rotation of the radiometer continuously adds energy to the air surrounding it, resulting in an accelerating rotation of air. The air continues to accelerate and reaches a velocity at which the input energy from rotation of the hub is equal to the viscous dissipation. At this point, air inside the box that houses the radiometer rotates at a constant velocity and the radiometer rotates within the rotating air. Hence, the absolute flow-through velocity becomes the rotational speed of the air plus flowthrough velocity as if the air was stationary. Finite element analysis presented in Fig 7a revealed the rotational speed of air to be between 10 and 20 mm/s. Since the model presented by Cortes et al. [4] for levitation of the single NCB assumes flight in stationary ambient air, we subtracted the average rotational speed of air inside a ring which the vanes sweep, from rotational speed of the radiometer to estimate for the flow through velocity that is compared with existing theory [4].

We hypothesize that surface effects in the boundary gas layers on the two sides of the nanocardboard play a significant role, which was neglected in Eq. 1. For example, the difference between the structure of the two surfaces, with CNTs on one side and ALD alumina on the other, result in different thermal interactions with the adjacent gas layers. One characteristic of thermal interaction is the thermal accommodation coefficient, α , [7] defined as

$$\alpha = \frac{T - T_{\infty}}{T_{\mathcal{S}} - T_{\infty}} \tag{7}$$

where T is the temperature of the gas molecules after thermal collision with the surface, and T_s and T_{∞} are the surface and ambient temperatures, respectively. The value of α depends on gas and surface properties and generally needs to be measured experimentally for any given gas/surface pair. Experimental studies on other surface-gas pairs, however, suggest that rougher surfaces have higher accommodation coefficients [8,9], meaning that carbon nanotubes likely have a higher accommodation coefficient. We believe that the discrepancy between the experimental and theoretical flow-through velocities may have been caused by the local temperature gradients due to different α values on the two sides, which our current theory does not consider. Occurrence of this phenomenon is owed to difference in molecular interaction between gas molecules and surfaces with different properties [9-11] and finite elements models are not capable of capturing such inetratctions. A detailed numerical study of this phenomenon requires Monte-Carlo method and molecular dynamics simulations of interactions between air, carbon nanotubes, and ALD deposited alumina. We encourage the research community to consider this as a research topic and contribute to our experimental demonstration of atmospheric radiometer.

VI. CONCLUSION

We have demonstrated, for the first time, a Crookes radiometer that can rotate at atmospheric pressure. This was made possible by making vanes out of a metamaterial called nanocardboard, which, compared to traditional paper vanes, was lighter, sustained a larger temperature gradient, and had a dense array of channels available for thermal transpiration. We characterized our radiometer using theoretical, numerical, and experimental approaches, obtaining qualitative agreement for the velocity of the vanes predicted by these approaches. Finally, we measured a maximum rotational velocity of close to 12 RPM at atmospheric pressure.

ACKNOWLEDGMENT

The authors thank Professor Howard Hu of the department of Mechanical Engineering and Applied Mechanics at the University of Pennsylvania for his help with the simulations and the staff of the Singh Center for Nanotechnology, Nanoscale Characterization Facility, and the Scanning and Local Probe facility at the same university, which are partly funded by the NSF National Nanotechnology Coordinated Infrastructure Program, under grant NNCI-1542153. This work was supported in part by the National Science Foundation (NSF) under CBET-

1845933, and the School of Engineering and Applied Science at the University of Pennsylvania.

REFERENCES

- A. Ketsdever, N. Gimelshein, S. Gimelshein, and N. Selden, "Radiometric phenomena: From the 19th to the 21st century", Vacuum 86, 1644-1662 (2012).
- [2] L.-H. Han, S. Wu, J. C. Condit, N. J. Kemp, T. E. Milner, M. D. Feldman, and S. Chen, "Light-powered micromotor: Design, fabrication, and mathematical modeling", Journal of Microelectromechanical Systems, 20, 487-496 (2011).
- [3] D. Wolfe, A. Larraza, and A. Garcia, "A horizontal vane radiometer: Experiment, theory, and simulation", Physics of Fluids, 28, 037103 (2016).
- [4] J. Cortes, C. Stanczak, M. Azadi, M. Narula, S. M. Nicaise, H. Hu, and I. Bargatin, "Photophoretic levitation of macroscopic nanocardboard plates", Advanced Materials 2020, 1906878 (2020).
- [5] B. M. Cornella, M. D. Ketsdever, N. E. Gimelshein, and S. F. Gimelshein, "Analysis of multivane radiometer arrays in high-altitude propulsion", Journal of Propulsion and Power, 28, 831-839 (2012).
- [6] C. Lin, S. M. Nicaise, D. E. Lilley, J. Cortes, P. Jiao, J. Singh, M. Azadi, G. G. Lopez, M. Metzler, P. K. Purohit, and I. Bargatin, "Nanocardboard as a nanoscale analog of hollow sandwich plates", Nature Communications 9, 4442 (2018).
- [7] F. O. Goodman, "Thermal accommodation coefficients", Journal of Physical Chemistry, 84, 1431-1445 (1980)
- [8] W. M. Trott, D. J. Rader, J. N. Castañeda, J. R. Torczynski, and M. A. Gallis, "Measurement of gas-surface accommodation" AIP conference proceedings 1084, 621 (2008)
- [9] M. Grau, F. Völklein, A. Meier, C. Kunz, J. Heidler, and P. Woias, "Method for measuring thermal accommodation coefficients of gases on thin film surfaces using a MEMS sensor structure" Journal of Vacuum Science and Technology A, 34, 041601 (2016)
- [10] P. Feuer "Theory of the thermal accommodation coefficients of a diatomic gas" J. Chem. Phys. 39, 1311 (1963)
- [11] W.M. Trott, D.J. Rader, J.N. Castaneda, J.R. Torczynski, and M.A. Gallis "Measurement of gas-surface accommodation" AIP Conference Proceedings 1084, 621 (2008)

BIOGRAPHICAL INFORMATION



Mohsen Azadi received his M.S.E. in mechanical engineering and applied mechanics from University of Pennsylvania (Philadelphia, PA, USA) in 2017 and his B.Sc. in mechanical engineering from Shiraz University (Shiraz, Fars, Iran) in 2013. He is currently pursuing his doctorate in mechanical

engineering and applied mechanics at the University of Pennsylvania.

He joined the Department of Mechanical Engineering and Applied Mechanics at the University of Pennsylvania as a Graduate Research Assistant in 2015 and served as a Teaching Assistant in the same department from 2016 to 2019. Prior to this, he was a Teaching Assistant at Shiraz University from 2012 to 2014 and was an Intern at the Fars Combined Cycle Power Plant (Fars, Iran) during the summer of 2013. His research interests include photophoretic levitation, microfabrication, and energy transformation.

Mr. Azadi received the Penn Prize for Excellence in Teaching by Graduate Students in 2019. In addition, he received the Mechanical Engineering and Applied Mechanics' Master of Science in Engineering Merit Scholarship in 2016, as well as the Singh Center for Nanotechnology Graduate Student Fellowship, also in 2016. He currently serves as a member of the Dean's Doctoral Advisory Board in the School of

Engineering and Applied Sciences at the University of Pennsylvania.



Zhipeng Lu received his B.S. in chemistry from Nanjing University (Nanjing, Jiangsu, China) in 2018. He is currently pursuing his doctorate in chemistry at the University of Pennsylvania (Philadelphia, PA, USA).

He joined the Department of Chemistry at the University of Pennsylvania as a

Graduate Research Assistant in 2018. From 2015 to 2018 he was an Undergraduate Researcher at the National Mesoscopic Laboratory (Nanjing, Jiangsu, China), where he coauthored several articles about perovskite solar cells. His current research interests include self-powering microdevices, thermal energy converters, and fluid mechanics. Mr. Lu received Nanjing University Elite Project scholarship from 2015 to 2017.



George A. Popov is currently pursuing joint degrees in mechanical engineering and applied mechanics (B.S.E.) and physics and astronomy (M.S., B.A.) with a concentration in Physical Theory and Experimental Techniques at the University of Pennsylvania (Philadelphia, PA, USA) as part of the Vagelos Integrated Program

in Energy Research.

He joined the Department of Mechanical Engineering and Applied Mechanics at the University of Pennsylvania as an Undergraduate Research Assistant in 2018. Prior to this, he worked as an Intern on a cold application-specific integrated circuit for the Deep Underground Neutrino Experiment as part of the Department of Physics and Astronomy at the University of Pennsylvania during the summer of 2017. In addition, he received the Victor W. K. Ku Memorial Award from the Department of Mechanical Engineering and Applied Mechanics at the University of Pennsylvania in 2020, and is a member of Tau Beta Pi. His current research interests include mechanical design, microelectromechanical systems devices, and energy applications.



Christopher Stanczak is currently pursuing a B.S.E. in Mechanical Engineering and Applied Mechanics and a B.A.S. in Physics at the University of Pennsylvania (Philadelphia, PA, US). He is part of the Vagelos Integrated Program in Energy Research at the University of Pennsylvania, which enables students to

pursue a coordinated dual-degree and provides funding for student research at Penn.

He joined the Bargain Research Group within the Department of Mechanical Engineering and Applied Mechanics in May of 2017 and has worked with the group as an Undergraduate Research Assistant for the past three years. His research interests include photophoretic levitation, energy science and transformation, and computational fluid dynamics.

Mr. Stanczak is a member of Phi Beta Kappa national honors society.



Andy G. Eskenazi is concurrently pursuing a B.S.E. in mechanical engineering and applied mechanics and a B.A. in mathematics at the University of Pennsylvania (Philadelphia, PA, USA). He is a participant in the Vagelos Integrated Program in Energy Research.

He joined the Department of Mechanical Engineering and Applied Mechanics at the University of Pennsylvania as an Undergraduate Research Assistant in 2019. In the 2019-2020 academic year, he also served as a Teaching Assistant for the introductory class in mechanical design in the same department. Prior to this, he engaged in a Chinese language program in Zhejiang University (Hangzhou, Zhejiang, China) in 2018, and completed his secondary education in Buenos Aires, Argentina, in 2017. His research interests include mechanical design, heat transfer, and sustainable energy technology.



Pratik Ponnarassery received his BE in Mechanical Engineering from Birla Institute of Technology and Science, Pilani (BITS Pilani) in 2019. He is currently pursuing his Master's in Mechanical Engineering and Applied Mechanics at the University of Pennsylvania.

He led a multi-disciplinary team of undergraduates in designing and fabricating a single seater race car to take part in FSAE competitions in India in 2018. Before joining UPenn, he interned at Mercedes Benz, R&D India in Bangalore. His research interests include fluid simulations, nano-scale materials, and energy transformation.



Dr. John Cortes earned his PhD in mechanical engineering and applied mechanics from University of Pennsylvania (Philadelphia, PA, USA) in 2019 and his B.S. in mechanical engineering from Clemson University in 2014. He is currently a mechanical engineering within the National Security

Engineering Division of the Lawrence Livermore National Laboratory (Livermore, CA, USA).

His graduate research focused on developing the capability to levitate ultralight, macroscopic plates using photophoresis as the source of propulsion.

Dr. Cortes earned the Graduate Assistance in Areas of National Need (GAANN) fellowship from the US Department of Education during his PhD studies at the University of Pennsylvania. He also won the 2016 Outstanding Teaching Assistant Award from the Department of Mechanical Engineering and Applied Mechanics at the University of Pennsylvania.



Matthew F. Campbell earned his Ph.D. and M.S. in mechanical engineering from Stanford University (Stanford, CA, USA) in 2014 and 2010, respectively, and his B.S.E. (*Magna cum laude* with distinction) in mechanical engineering and materials science from Duke University (Durham, NC, USA) in 2008. He also obtained his

professional engineering licensure (P.E.) in mechanical engineering in the state of California in 2014 and a certificate in markets and management studies from Duke University in 2008.

From 2014 to 2016 he was a Postdoctoral Appointee at Sandia National Laboratories (Livermore, CA, USA), and from 2017 to 2019 he worked as an Engineer and Educator with a nonprofit organization on the campus of Mindanao State University (General Santos City, Philippines). In 2019, he began working as a Postdoctoral Researcher in the Department of Mechanical Engineering and Applied Mechanics at the University of Pennsylvania (Philadelphia, PA, USA). His research include interests energy transformation, micromanufacturing, and thermal-fluid science. He has served as a referee for seven peer-reviewed publications, including Combustion and Flame, Energy & Fuels, and Proceedings of the Combustion Institute.

Dr. Campbell received the National Defense Science and Engineering Graduate (NDSEG) fellowship from 2010 to 2013. He is a member of Phi Beta Kappa, Tau Beta Pi, and Pi Tau Sigma.



Igor Bargatin earned his Ph.D. in physics and electrical engineering in 2008 at the California Institute of Technology (Pasadena, CA, USA) and his B.S. in theoretical physics in 2000 from M. V. Lomonosov Moscow State University (Moscow, Russia).

From 2008 to 2012 he was a Postdoctoral Researcher in the Department of Electrical Engineering at Stanford University (Stanford, CA, USA), after which he joined the faculty in the Department of Mechanical Engineering and Applied Mechanics at the University of Pennsylvania (Philadelphia, PA, USA) in 2013 as the Class of 1965 Term Assistant Professor. He was thereafter promoted to Associate Professor in the same department in 2020. His research interests involve mechanical metamaterials, solid-state energy converters, and micro- and nanoelectromechanical systems.

Professor Bargatin was the recipient of a 2019 NSF CAREER Award for a project to enable macroscopic levitation of ultrathin metamaterials. He also received the University of Pennsylvania School of Engineering and Applied Science S. Reid Warren, Jr. Teaching Award in 2019 in recognition of his outstanding service in stimulating and guiding the intellectual and professional development of undergraduate students.